Recombination dynamics and screening of the internal electric field in $ZnO/Zn_xMg_{1-x}O$ multiple quantum wells

C. R. Hall,[1] L. Dao,[1] K. Koike,[2] S. Sasa,[2] H. H. Tan,[3] M. Inoue,[2] M. Yano,[2] P. Hannaford,[1] C. Jagadish,[3] and J. A. Davis[1]
[1]*Centre for Atom Optics and Ultrafast Spectroscopy, Swinburne University of Technology, Melbourne 3122, Australia*
[2]*Nanomaterials Microdevices Research Center, Osaka Institute of Technology, Asahi-ku Ohmiya, Osaka 535-8585, Japan*
[3]*Department of Electronic Materials Engineering, Research School of Physical Sciences and Engineering, The Australian National University, Canberra, Australian Capital Territory 0200, Australia*
(Received 29 September 2009; revised manuscript received 12 November 2009; published 15 December 2009)

We investigate the recombination dynamics within screened *c*-axis $ZnO/Zn_{0.7}Mg_{0.3}O$ quantum wells using time-resolved photoluminescence and femtosecond pump-probe spectroscopy. The relaxation of excited carriers restores the strength of the internal electric field, which we follow, via the decay time constant, as it increases from 180 ns to 5.8 μs. Pump-probe spectroscopy reveals faster, initial decay times of 160–250 ps, which we attribute to additional recombination mechanisms, that become significant for carrier densities greater than 2×10^{12} pairs cm^{-2}. In addition, the time for screening of the internal electric field to be established is measured to be less than 1 ps. These measurements are followed by a self-consistent calculation which solves the Schrödinger and Poisson equations for pair densities up to 1×10^{13} pairs cm^{-2}, where there is no further substantial blueshifting of the transition energy with increasing pair density because the electron and hole charge distributions cancel. This calculation fits the measured recombination dynamics and can be used to determine the quantum-well properties at any time following excitation, including carrier densities, transition energies, and recombination lifetimes.

DOI: 10.1103/PhysRevB.80.235316 PACS number(s): 78.47.−p, 78.55.Et, 78.67.De

I. INTRODUCTION

ZnO is a wide band-gap semiconductor that has properties suited for applications within devices optically active in the UV region,[1–3] some of which make ZnO preferable to GaN, its established and main competitor.[2] Of particular interest are the superior exciton and biexciton binding energies (ZnO 60 and 15 meV, GaN 25 and 5.3 meV, respectively),[4–6] which give advantages to ZnO over GaN when considering oscillator strength and efficient light absorbing/emitting devices.[7]

By integrating these materials into quantum-well (QW) structures, not only is there the opportunity to tune the transition energy but also the exciton and biexciton binding energies can be even larger; hence these structures are of considerable interest.[8,9] Growth of ZnO/ZnMgO quantum wells is preferentially *c*-axis oriented, which, to the detriment of a number of properties, leads to an internal electric field across the quantum well and the quantum-confined Stark effect (QCSE). This internal electric field arises as a result of mismatches in the spontaneous and piezoelectric polarizations of the well and barrier materials.[10–12] In sufficiently wide wells, this internal electric field redshifts the quantum-well transition energy below the bulk ZnO transition and spatially separates excited-state electrons and holes, consequently reducing the oscillator strength and decreasing the rate of recombination. As the width of the well increases so does the separation of the electron and hole wave functions for the E1–H1 transition (the primary radiative recombination pathway), producing even longer excited-state lifetimes.[13] It has been shown that the exciton binding energies are also reduced as the well width is increased.[14] When a large population of excited carriers is generated within such QWs, the internal electric field will be shielded, blueshifting the transition energy and increasing the recombination rate. In addition, given the large carrier densities, the possibility of crossing the Mott transition should also be considered, in which case an even faster rate of recombination proportional to electron-hole wave-function overlap would be observed.[15] However, the exact density for the observation of the Mott transition is unknown given the quantum-well potential profile changes with carrier density.

To date, work on the QCSE in ZnO quantum wells has been limited to a number of photoluminescence (PL) measurements and fewer time-resolved measurements which have not looked at subnanosecond time scales in great detail.[14,16–21] In this paper we examine the screening dynamics within wide ZnO QWs, including short-time dynamics, employing PL, time-resolved PL (TRPL), and femtosecond pump-probe (PP) spectroscopy. Using self-consistently solved Schrödinger and Poisson equations we model the recombination dynamics within such a structure and compare with experimental results.

II. EXPERIMENT

The sample examined is a $ZnO/Zn_{0.7}Mg_{0.3}O$ multiple quantum well (MQW) made of six quantum wells of width 6 nm and barriers of 5.5 nm grown by molecular-beam epitaxy. A 30% Mg composition is used in the barrier to maximize the strength of the internal electric field. The large barrier width is intended to reduce carrier-induced shielding by adjacent wells. The electric field within the QWs in this sample has been determined previously to be 0.8 MV cm^{-1}, reduced from 0.9 MV cm^{-1} due to the so-called geometric effect.[13]

Both PL and PP experiments were carried out with 100 fs laser pulses at a repetition rate of 1 kHz. Two synchronously pumped optical parametric amplifiers were used to tune the

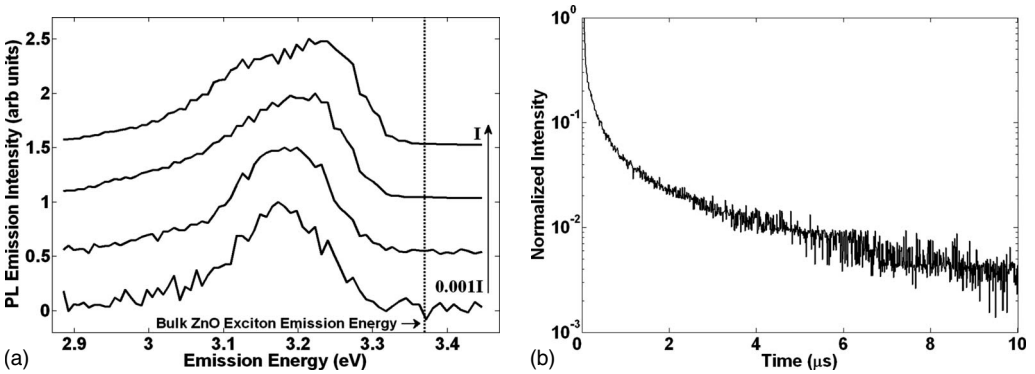

FIG. 1. (a) Intensity-dependent PL at 20 K for intensities 0.001*I*, 0.01*I*, 0.1*I*, and *I* (bottom to top). Over 3 orders of magnitude of incident intensity, the PL peak emission blueshifts 66 meV. The bulk ZnO exciton emission energy at 20 K (Ref. 25) is included to demonstrate the substantial redshift of the QW transition energy due to the internal electric field. (b) Time-resolved PL at 20 K.

photon energy from 4.96 to 3.26 eV in these experiments. The TRPL measurements were made using a PMT and a 500 MHz oscilloscope. For all results discussed here the sample was maintained at a temperature of 20 K.

III. EXPERIMENTAL RESULTS

The intensity dependence of the PL for this sample at 4.96 eV with a maximum excitation of 4×10^{15} photons cm^{-2} per pulse is shown in Fig. 1(a). As a pulsed laser was used as the excitation source, the spectra appear somewhat different to previously reported results that have used continuous-wave (cw) excitation.[14,21] When cw excitation is used, a constant excited-state population can be sustained, which in turn maintains a constant shielding magnitude within the QW. A narrow peak that can be blueshifted by an amount proportional to the excitation intensity is observed. In our case, where pulsed excitation is used, the excited-state population decays before the arrival of successive pulses. The decaying population progressively restores the internal electric field, which in turn redshifts the transition energy. Time-integrated detection consequently records a peak that appears broad but represents emission from a shifting transition over a continuous range of screening magnitudes from some initial carrier density that decays to zero.[22]

The excitation intensity in Fig. 1(a) is varied over 3 orders of magnitude and a significant blueshift of the peak emission (~66 meV) with increasing intensity is observed due to screening of the internal electric field. There is also increased broadening on the low-energy side of the PL peak, which is attributed to an enhanced longitudinal-optical phonon-exciton coupling that is manifested in strong phonon replica peaks (a well-known characteristic of spatially separated electron-hole pairs[18]) and collisional broadening associated with the high carrier densities present within the quantum well.

Figure 1(b) shows the time-resolved PL, where care was taken to keep the signal strength well within the linear-response range of the PMT. The measured signal is clearly nonexponential and continuously varying up to a seemingly steady rate of decay with a relatively long lifetime, more than an order of magnitude larger than the initial rate of decay. The continuously changing lifetime can be explained as follows: for a large initial carrier density there is substantial screening of the internal electric field but as excited-state carriers gradually recombine the amount of screening is reduced. This restores the magnitude of the internal electric field, which in turn decreases the electron and hole wave-function overlap, resulting in increased carrier lifetimes. The changing lifetime of this system is described by the relationship[15]

$$\tau(n) = \tau(0)\left\{\left[\int_{-\infty}^{\infty}\psi_e(0)\psi_h(0)dz\right]^2 / \left[\int_{-\infty}^{\infty}\psi_e(n)\psi_h(n)dz\right]^2\right\}, \quad (1)$$

where $\tau(0)$ is the lifetime of the unscreened QW and $[\int_{-\infty}^{\infty}\psi_e(n)\psi_h(n)dz]$ is the electron and hole overlap integral as a function of carrier density. Table I presents the time constants for single exponential decays fit to successive periods over the decay curve presented in Fig. 1(b), and for two other emission energies (curves not shown). It is evident that as the excited population decays over time, the lifetime of the measured decay grows. Over this measurement, the de-

TABLE I. Single exponential decay time constants for various sections of TRPL decay curves. The initial decay portion (star) is excluded because of laser scatter (40 ns detector response).

Period (μs)	Decay time constant (μs)
0–0.04	⋆
0.04–0.14	0.18
0.14–0.24	0.27
0.24–0.34	0.34
0.34–0.44	0.41
0.44–1	0.75
1.0–2.0	1.57
2.0–3.0	2.3
3.0–4.0	3.91
4.0–5.0	5.8

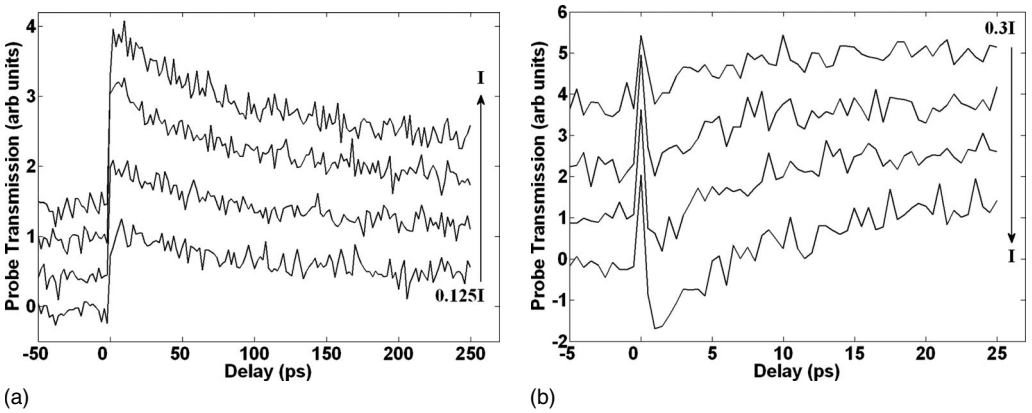

FIG. 2. (a) Pump-probe measurement with pump and probe at 3.28 eV. Substantially different decay times over the period 0–100 ps are observed for different pump intensities. The pump intensities increase from bottom to top with the following lifetimes; 157 ps, (0.5*I*) 167 ps, (0.25*I*) 199 ps, and (0.125*I*) 245 ps. (b) Pump (3.28 eV) with probe (3.34 eV) shows an initial absorption which is strongest for the largest intensities (pump intensity increases from top to bottom in the order 0.3*I*, 0.5*I*, 0.8*I*, and *I*.

cay time constant increases from 180 ns to 5.8 μs after a period of 5 μs.

In order to examine the dynamics of the carrier-induced shielding of the internal electric field in the same ZnO MQW on a faster time scale we have used PP spectroscopy. Given that screening of the internal electric field is carrier induced, we have varied the pump intensity to examine the carrier-density-dependent screening dynamics. A maximum excitation intensity of $I=2.5\times10^{17}$ photons cm^{-2} per pulse was used.

Figure 2(a) shows the transmitted probe signal for a pump of varying intensity. The pump and probe photon energies are tuned to be slightly blue of the high intensity PL peak with a photon energy of 3.28 eV and below the band gap of bulk ZnO to ensure that any observed dynamics are from the quantum well. From this data it is evident that at early times the decay rate increases with increasing excitation intensity. This is confirmed by fitting a single exponential to the data in the period 0–100 ps, which gives decay time constants of 160 ± 20, 170 ± 20, 200 ± 30, and 250 ± 80 ps for intensities *I*, 0.7*I*, 0.5*I*, and 0.25*I*, respectively. This result will be examined further in the discussion section.

Figure 2(b) shows PP results with a probe energy of 3.34 eV and an unchanged pump energy of 3.28 eV. In contrast to the results in Fig. 2(a), for a high excitation intensity an initial transient absorption is observed which evolves into a transient transmission with a long decay (not shown), much like the one observed in Fig. 2(a). As the excitation intensity is reduced from *I* to 0.5*I*, the absorption becomes weaker, until finally, at 0.3*I*, there is no longer evidence of absorption. The transient absorption is attributed to the quantum-well exciton transition being blueshifted, becoming resonant with the probe photon energy and increasing the density of available states at this energy. A time constant of 7 ps is measured for the transition from absorption to the long-lived bleach and corresponds to the time it takes for the transition energy to shift out of resonance with the probe photon energy. For probe energies greater than 3.34 eV, no signal is observed, suggesting this is the highest energy to which the transition shifts following this excitation. The almost immediate onset of the transient absorption shows that the shielding of the internal electric field by carriers generated within the quantum wells is an extremely fast process (<1 ps). This is consistent with the theory work of Turchinovich *et al.*[22,23] which shows that the maximum absorption should occur within the duration of the excitation pulse as the excited carriers are produced in instantaneously polarized states.

IV. SIMULATION

In order to verify our interpretation thus far, and provide some additional insight concerning the changing quantum-well properties, we have calculated the extent of shielding and the effect on transition energy and lifetime due to a large excited-state population. The simplest way to calculate the carrier-induced shielding within a quantum well with an internal electric field would be to assume that all excited carriers are localized at the interfaces, and thereby simply altering the slope of a triangular potential profile. Calculating the change in shape of the potential profile due to the spatially dependent accumulation of charges, however, will provide a more accurate result, especially in considering the pair-density-dependent wave-function overlap.[24] This can be achieved by solving the Schrödinger and Poisson equations self-consistently. Our calculation determines the spatially dependent QW potential for an incrementally increasing excited pair density which is then used to determine the pair-density-dependent transition energy and electron-hole wave-function overlap. This is then used to analyze the experimentally measured recombination dynamics. Our method is based on that described by Lefebvre *et al.*[24]

Figure 3 plots the calculated quantum-well transition energy as a function of pair density. The quantum-well transition energy for the unscreened quantum well was calculated to be 3.175 eV, which compares well with our experimentally measured value of 3.17 eV for low excitation intensity. It is revealed that for pair densities up to 1×10^{11} pairs cm^{-2} there is only a very slight increase in the transition energy. Between 1×10^{11} and 1×10^{12} pairs cm^{-2} we see an increase in the quantum-well

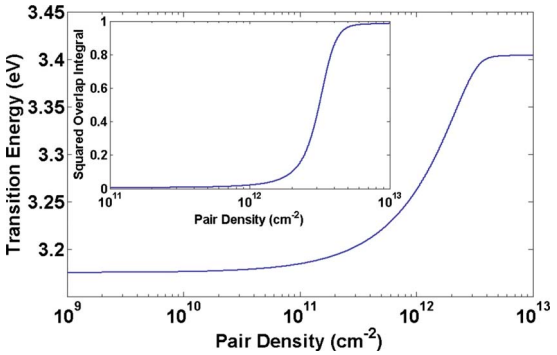

FIG. 3. (Color online) Quantum-well transition energy as a function of carrier pair density. Inset: E1–H1 wave-function squared overlap integral as a function of pair density.

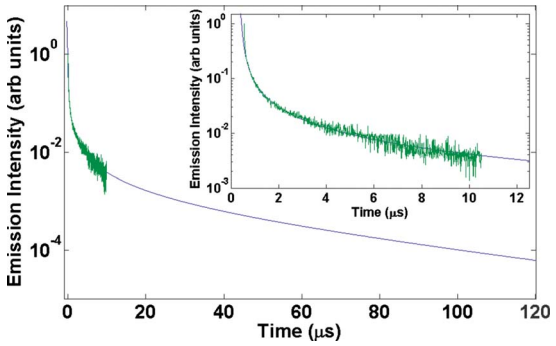

FIG. 4. (Color online) The recreated recombination dynamics from the pair-density-dependent wave-function overlap fit to the TRPL curve from Fig. 2. Inset, a closeup of the fit at early times.

transition energy from 3.18 to 3.25 eV. The most significant increase in transition energy, however, occurs from 1×10^{12} to 4.2×10^{12} pairs cm^{-2}, where the transition energy shifts from 3.25 eV and plateaus at 3.40 eV. The plateau appears when additional excited pairs produce no significant change in the shape of the potential profile because the electron and hole wave functions of additional pairs overlap and their charge distributions cancel.

The square of the electron and hole wave-function overlap integral as a function of pair density is shown in the inset of Fig. 3. From this, the recombination dynamics as a function of pair density can be determined using[24]

$$\frac{dn}{dt} = -\frac{n}{\tau(n)}, \tag{2}$$

where n is the pair density and $\tau(n)$ is the density-dependent lifetime determined from the electron-hole overlap integral using Eq. (1).

We have calculated the recombination dynamics using Eq. (2) and the data presented in Fig. 3. However, there is no point of reference to scale the calculated recombination dynamics given that we cannot assume the longest measured decay time constant corresponds to the unscreened quantum-well lifetime (because the measured signal is limited by detector sensitivity and the lifetime continues to evolve beyond this point), and we do not know the initial carrier density without guessing the QW capture efficiency. We have therefore chosen to fit this result to the experimental TRPL using

$$S_{\mathrm{FIT}} = A \times S_{\mathrm{CALC}}[(t)\times T + t_0], \tag{3}$$

where S_{CALC} represents the calculated decay curve as a function of delay; A is the amplitude scaling factor, which corresponds to the detection efficiency; T is the scaling factor for the time axis and effectively fits for τ_0, the unscreened lifetime; and t_0 offsets the calculated decay curve to correct for the initial pair density within the QW immediately following excitation. The fitting error is determined from the relative difference between the calculated and measured curves.

The resulting calculated recombination dynamics are shown in Fig. 4 and fit remarkably well to the experimental data. Using this result the carrier-density-dependent properties of the quantum wells can be determined at any time following excitation. The only significant discrepancy for the fit occurs at the beginning of the experimentally measured decay (inset Fig. 4) where there is an initial fast decay of 40 ns in duration. This signal is most likely due to laser scatter, the duration of which is limited by the response time of the detection, and was excluded from the fitting process.

The fitting process was able to provide a unique solution with a global minimum in the error metric. The range of values quoted for the parameters in the following discussion are given for the greatest variation within 3% of the global minimum.

V. DISCUSSION

In the above calculation, the pair-density-dependent wave-function overlap was used with Eq. (2) to determine some of the quantum-well properties as they evolve in time, specifically, the E1–H1 transition energy, the recombination lifetime, and the excited-state pair density.

Extrapolating the fit, Fig. 4, back to the beginning of the measured decay predicts an initial pair density of 2.38×10^{12} to 2.69×10^{12} cm^{-2}. The incident photon density is 4×10^{15} cm^{-2} and suggests a reasonable QW capture efficiency of 0.06–0.074 % per well following excitation high into the QW barrier.

Additionally, this pair density corresponds to a QW transition energy of 3.357–3.372 eV, as shown in Fig. 3. The PL results in Fig. 1(a) actually show emission up to 3.35 eV although it is not as strong as might be expected. To explain this we consider two possibilities: first, there may be increased nonradiative recombination at large carrier densities. This suggests that for early times, beyond the resolution of the TRPL experiments, additional processes may lead to a deviation from the calculated curve, and greater uncertainty in the initial pair density. Another possible explanation is that the effects of band-gap renormalization, which have not been included in the transition-energy calculation, may be significant at the high carrier densities present shortly after excitation. This may redshift the transition energy by up to several tens of meV and explains the lack of emission at high energy. If this is the case, then the calculated transition energy as a function of pair density would be overestimated, particularly for large densities; the calculated wave-function overlap and

lifetimes, however, would not be affected. Unfortunately, band-gap renormalization in this case is difficult to calculate because of the continuously changing potential profile. In addition, there does not seem to be any detailed publications giving typical values for band-gap renormalization in ZnO/ZnMgO quantum wells.

At 5 μs following excitation, a pair density of 9.2×10^{11} to 7.1×10^{11} cm^{-2} remains within each QW giving a transition energy of 3.256–3.237 eV (the transition-energy discrepancy due to band-gap renormalization will be minimal). The decay time constant for this pair density is calculated to be 4.5–4.38 μs and agrees with the measured value of 5.8 ± 2 μs. As there is still a substantial excited-state population within the QWs at this point, it is clear that these values cannot represent the lifetime of the unshielded QWs. According to the calculation, τ_0, the lifetime in the unshielded well, is 34 ± 9 μs. Based on these values for τ_0 and using Eq. (1), we may determine the fastest decay time constant for this sample (assuming the pair density is below the Mott transition) in the event of complete wave-function overlap to be 1–2 ns (where the unshielded well-squared overlap integral is 0.0048).

Returning to the pump-probe results in Fig. 2(a), initial decay times from 157 to 245 ps, dependent on excitation intensity, were observed, shorter than the 1–2 ns predicted. In Fig. 2(a), the initial periods of decay occur on top of a decay with a much longer time constant. We attribute this long lifetime to behavior consistent with the TRPL experiments and calculations. The rapidly decaying part of the signal is then attributed to an increase in nonradiative recombination at the initial high pair densities. This is further confirmed by the elimination of the fast component for lower excitation intensities. An alternative explanation that cannot be ruled out is that the increased rate of decay at early times is due to the density exceeding the Mott density. Regardless, the density required for this nonlinear behavior to be present is greater than 2.1×10^{12} cm^{-2} (from Fig. 3), although this value may be underestimated due to band-gap renormalization being excluded from the calculations.

VI. SUMMARY

In summary, we have studied the recombination dynamics within 6 nm ZnO/ZnMgO QWs. The presence of carrier-induced shielding is evidenced by blueshifting of the PL peak with excitation intensity and in TRPL by a decay constant that increases as the system evolves in time by more than an order of magnitude from an initial decay time of 180 ns. The recombination dynamics were calculated and fit to the TRPL, from which we determined the pair density at any point following excitation and predicted the asymptotic lifetime of the unshielded well to be 34 ± 9 μs. The calculated transition energies, however, are overestimated, as the extent of band renormalization in ZnO quantum wells is unknown. Pump-probe spectroscopy measured faster initial recombination times, from 160 to 250 ps, due to additional recombination pathways that become important for carrier densities greater than 2.1×10^{12} pairs cm^{-2}. These possibly include nonradiative recombination and/or an increased radiative recombination due to having exceeded the Mott-transition density. On even shorter time scales we observed a rapidly established absorption, the screening establishment time, which was measured to take less than 1 ps.

ACKNOWLEDGMENTS

The authors gratefully acknowledge the support of the Australian Research Council. C.R. Hall would also like to thank Lastek for their financial support.

[1] D. C. Look, Mater. Sci. Eng., B **80**, 383 (2001).
[2] Ü. Özgür, Y. I. Alivov, C. Liu, A. Teke, M. A. Reshchikov, S. Dogan, V. Avrutin, S. J. Cho, and H. Morkoc, J. Appl. Phys. **98**, 041301 (2005).
[3] A. Tsukazaki, A. Ohtomo, T. Onuma, M. Ohtani, T. Makino, M. Sumiya, K. Ohtani, S. F. Chichibu, S. Fuke, Y. Segawa, H. Ohno, H. Koinuma, and M. Kawasaki, Nature Mater. **4**, 42 (2005).
[4] K. Okada, Y. Yamada, T. Taguchi, F. Sasaki, S. Kobayashi, T. Tani, S. Nakamura, and G. Shinomiya, Jpn. J. Appl. Phys., Part 2 **35**, L787 (1996).
[5] J. W. Orton and C. T. Foxon, Rep. Prog. Phys. **61**, 1 (1998).
[6] C. Jagadish and S. J. Pearton, *Zinc Oxide Bulk, Thin Films and Nanostructures* (Elsevier, Oxford, 2006).
[7] J. A. Davis and C. Jagadish, Laser Photonics Rev. **3**, 85 (2009).
[8] H. D. Sun, T. Makino, N. T. Tuan, Y. Segawa, Z. K. Tang, G. K. L. Wong, M. Kawasaki, A. Ohtomo, K. Tamura, and H. Koinuma, Appl. Phys. Lett. **77**, 4250 (2000).
[9] C. H. Chia, T. Makino, K. Tamura, Y. Segawa, M. Kawasaki, A. Ohtomo, and H. Koinuma, Appl. Phys. Lett. **82**, 1848 (2003).
[10] S. H. Park and S. L. Chuang, Appl. Phys. Lett. **76**, 1981 (2000).
[11] T. Bretagnon, P. Lefebvre, T. Guillet, T. Taliercio, B. Gil, and C. Morhain, Appl. Phys. Lett. **90**, 201912 (2007).
[12] M. Yano, K. Hashimoto, K. Fujimoto, K. Koike, S. Sasa, M. Inoue, Y. Uetsuji, T. Ohnishi, and K. Inaba, J. Cryst. Growth **301-302**, 353 (2007).
[13] J. A. Davis, L. V. Dao, X. Wen, C. Ticknor, P. Hannaford, V. A. Coleman, H. H. Tan, C. Jagadish, K. Koike, S. Sasa, M. Inoue, and M. Yano, Nanotechnology **19**, 055205 (2008).
[14] C. Morhain, T. Bretagnon, P. Lefebvre, X. Tang, P. Valvin, T. Guillet, B. Gil, T. Taliercio, M. Teisseire-Doninelli, B. Vinter, and C. Deparis, Phys. Rev. B **72**, 241305(R) (2005).
[15] S. Kalliakos, P. Lefebvre, and T. Taliercio, Phys. Rev. B **67**, 205307 (2003).
[16] T. Makino, K. Tamura, C. H. Chia, Y. Segawa, M. Kawasaki, A. Ohtomo, and H. Koinuma, Appl. Phys. Lett. **81**, 2355 (2002).
[17] T. Makino, A. Ohtomo, C. H. Chia, Y. Segawa, H. Koinuma, and M. Kawasaki, Physica E (Amsterdam) **21**, 671 (2004).
[18] T. Bretagnon, P. Lefebvre, P. Valvin, B. Gil, C. Morhain, and X. Tang, J. Cryst. Growth **287**, 12 (2006).

[19] T. Guillet, T. Bretagnon, T. Taliercio, P. Lefebvre, B. Gil, C. Morhain, and X. Tang, Superlattices Microstruct. **41**, 352 (2007).
[20] B. P. Zhang, B. L. Liu, J. Z. Yu, Q. M. Wang, C. Y. Liu, Y. C. Liu, and Y. Segawa, Appl. Phys. Lett. **90**, 132113 (2007).
[21] T. Makino, Y. Segawa, A. Tsukazaki, A. Ohtomo, and M. Kawasaki, Appl. Phys. Lett. **93**, 121907 (2008).
[22] D. Turchinovich, P. U. Jepsen, B. S. Monozon, M. Koch, S. Lahmann, U. Rossow, and A. Hangleiter, Phys. Rev. B **68**, 241307(R) (2003).
[23] D. Turchinovich and P. U. Jepsen, Phys. Status. Solidi C **3**, 2494 (2006).
[24] P. Lefebvre, S. Kalliakos, T. Bretagnon, P. Valvin, T. Taliercio, B. Gil, N. Grandjean, and J. Massies, Phys. Rev. B **69**, 035307 (2004).
[25] A. Teke, Ü. Özgür, S. Dogan, X. Gu, H. Morkoc, B. Nemeth, J. Nause, and H. O. Everitt, Phys. Rev. B **70**, 195207 (2004).